

Mechanisms for enhanced supercurrent across meandered grain boundaries in high-temperature superconductors

D. M. Feldmann^{a)}

University of Wisconsin-Madison, Madison, Wisconsin 53706, USA

T. G. Holesinger

Los Alamos National Laboratory, Los Alamos, New Mexico 87545, USA

R. Feenstra and C. Cantoni

Oak Ridge National Laboratory, Oak Ridge, Tennessee 37831, USA

W. Zhang, M. Rupich, and X. Li

American Superconductor, 2 Technology Drive, Westborough, Massachusetts 01581, USA

J. H. Durrell

Cambridge University, Pembroke Street, Cambridge CB2 3QZ, United Kingdom

A. Gurevich^{b)} and D. C. Larbalestier^{b)}

University of Wisconsin-Madison, Madison, Wisconsin 53706, USA

(Received 6 August 2007; accepted 2 September 2007; published online 24 October 2007)

It has been well established that the critical current density J_c across grain boundaries (GBs) in high-temperature superconductors decreases exponentially with misorientation angle θ beyond $\sim 2^\circ - 3^\circ$. This rapid decrease is due to a suppression of the superconducting order parameter at the grain boundary, giving rise to weakly pinned Abrikosov-Josephson (AJ) vortices. Here we show that if the GB plane meanders, this exponential dependence no longer holds, permitting greatly enhanced J_c values: up to six times at 0 T and four times at 1 T at $\theta \sim 4^\circ - 6^\circ$. This enhancement is due to an increase in the current-carrying cross section of the GBs and the appearance of short AJ vortex segments in the GB plane, confined by the interaction with strongly pinned Abrikosov (A) vortices in the grains. © 2007 American Institute of Physics. [DOI: 10.1063/1.2800255]

INTRODUCTION

The complex behavior of grain boundaries (GBs) in high-temperature superconductors (HTSs) is still not well understood because of the interplay of many competing mechanisms, such as the d -wave pairing symmetry, impurity scattering, hole nonstoichiometry, nanoscale phase separation due to the order parameter suppression, and precipitation of the antiferromagnetic dielectric phase augmented by charging and strain effects produced by the chain of GB dislocations.¹ Moreover, the suppression of superconductivity on charged dislocation cores and in nanoscale channels between them makes GBs strong barriers to current flow,^{1–3} a fact that has remained one of the most significant challenges to applications of HTSs.⁴ As shown by Dimos *et al.* in 1990,⁵ and many times confirmed,^{1,6,7} the critical current density J_c across GBs in $\text{YBa}_2\text{Cu}_3\text{O}_{7-\delta}$ (YBCO) falls off exponentially below the intragrain J_c beyond a certain critical misorientation angle θ_c . While the data of Dimos *et al.* suggested θ_c as large as 10° , more recent work confirms θ_c to be no larger than $2^\circ - 3^\circ$.^{6,7} It has been shown that dislocations which form low angle GBs act as pinning centers for the hybrid Abrikosov-Josephson (AJ) vortices at the grain boundary.^{8,9}

Knowledge of GB transport properties has been based largely on extensive investigations of YBCO films grown by

pulsed laser deposition (PLD) on SrTiO_3 (STO) bicrystal substrates^{1,5,7} for which GBs are macroscopically planar and parallel to the film normal. However, in certain *ex situ* growth processes,¹¹ qualitatively different grain boundary interfaces can occur.^{12,13} Thick ($>0.5 \mu\text{m}$) *ex situ* processed films exhibit extensive GB meandering both through the thickness of the film and in the plane of the film.^{12,13} In this case the surface between two grains is no longer planar but often becomes fractal or reentrant with amplitudes up to ten times larger than the film thickness¹³ due to the lateral growth mode of the grains induced by precipitation from a transient liquid phase.¹⁴ The meandering of the GB radically changes mechanisms of intergrain current transport in HTS, as shown below.

Unlike nominally planar GBs in PLD films, a detailed study of transport properties has not been previously performed for meandered GBs. We report here on the $J_c(\theta, H)$ dependence of strongly meandered YBCO GBs in thick ($\sim 0.8 \mu\text{m}$) *ex situ* processed films and find significant enhancements of $J_c(\theta, H)$ as compared to planar GBs. We attribute this enhancement to an increase in GB area and the effective suppression of the channeling of weakly pinned vortex segments along the GB due to their confinement by strongly pinned vortices in the grains. Our results show that there are circumstances under which the criteria of Dimos *et al.*⁵ do not hold and that a radical reduction of current-blocking effects of grain boundaries in HTS can be achieved without complex doping of GBs [i.e., Ca. (Ref. 15)].

^{a)}Present address: Los Alamos National Laboratory, Los Alamos, NM 87545.

^{b)}Present address: National High Magnetic Field Laboratory, Florida State University, 2031 E. Paul Dirac Drive, Tallahassee, FL 32310.

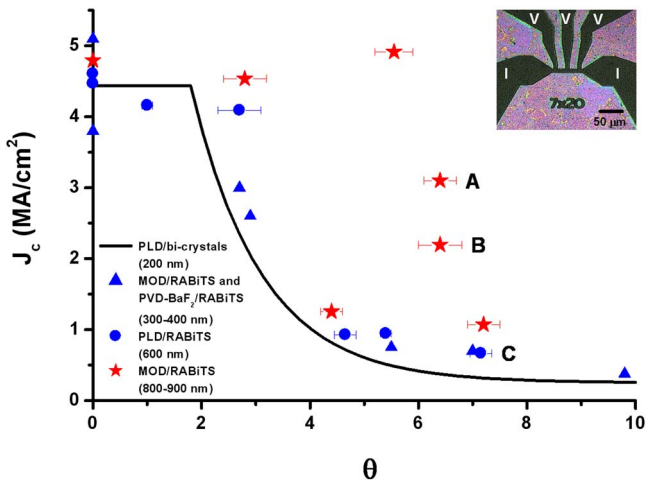


FIG. 1. (Color online) J_c as a function of θ for several types of YBCO films. The data were acquired at 77 K and self-field (zero applied field). J_c was calculated by dividing the critical current of the link by the cross-sectional area of the link. Data plotted at $\theta=0$ represent the critical current density of the grain. The inset is a light microscope image of an isolated GB (right link) and an adjacent grain (left link) in a MOD/RABiTS sample; current and voltage taps are highlighted and the same circuit was used to measure all samples in this work.

EXPERIMENTAL

Single GBs in YBCO films were isolated in samples featuring polycrystalline rolling assisted biaxially textured substrates (RABiTSs).¹⁶ Specific architectures were YBCO (600–800 nm)/CeO₂ (55–75 nm)/yttria-stabilized zirconia 75–200 nm/Y₂O₃ (30–75 nm)/Ni–5% W (75 μ m) with an average Ni–W (RABiTS) grain size of $\sim 25 \mu$ m. The YBCO was deposited by both PLD and the *ex situ* metalorganic deposition (MOD) process.¹⁷ Electron backscatter diffraction (EBSD) data were used to identify the GBs in the YBCO, and grains and GBs of specific θ were then chosen for study and measured with 7 μ m wide, 20 μ m long links defined by standard photolithography methods. Four-probe measurements of dc voltage-current characteristics with <0.2 nV noise level allowed us to report J_c values at the 1 uV/cm electric field criterion (2 nV). Transmission electron microscopy (TEM) images were taken on a Tecnai TF30 TEM/scanning TEM microscope operating at 300 kV.

RESULTS AND DISCUSSION

Figure 1 presents the self-field $J_c(\theta)$ dependence for several types of YBCO films: 200 nm thick PLD-grown films on [001] tilt STO bicrystals taken from Verebelyi *et al.*⁷ (solid line), 300–400 nm thick *ex situ* processed films grown by either the physical vapor deposition-BaF₂ (PVD-BaF₂) method or MOD on RABiTS (triangles, data taken from Feldmann *et al.*,⁶ 600 nm thick PLD-grown films on RABiTS (circles, this work), and 800 nm thick MOD-grown films on RABiTS templates, single GBs were isolated and measured as described above. As previously reported, 300–400 nm thick PVD-BaF₂ and MOD-grown films do not result in significant GB meandering.¹² No significant GB meandering is observed in the 600 nm thick PLD-grown films on RABiTS either, as shown in Fig. 2(a). These two data sets fit remark-

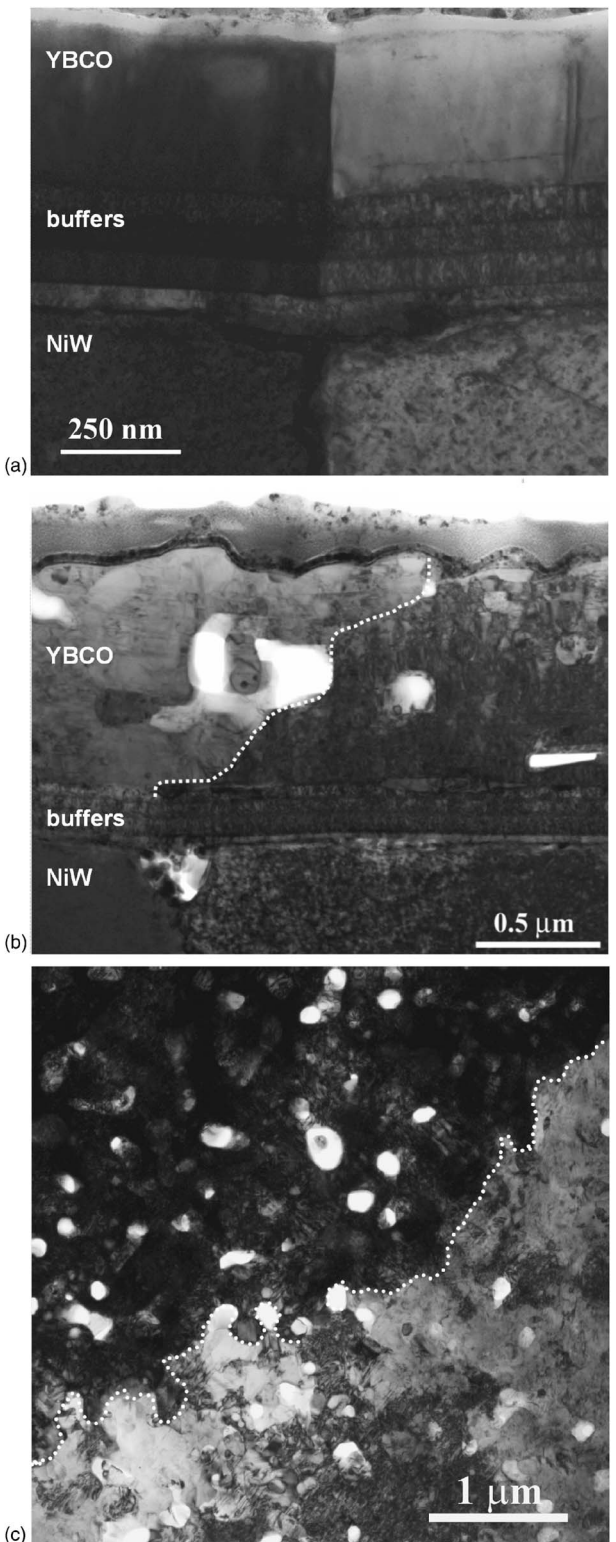


FIG. 2. TEM images of GBs in YBCO films on RABiTS. (a) A cross-sectional TEM image revealing a planar GB in a PLD-grown film. (b) A cross-sectional TEM image revealing a meandered GB in a MOD-grown film. (c) A plan-view TEM image of a meandered YBCO GB in a MOD-grown film. The GBs of (a) and (b) were first isolated within 7 μ m wide links and characterized electromagnetically, and then TEM specimens were prepared from within these links with a focused ion beam. The GB $J_c(77 \text{ K}, 0 \text{ T})$ values were (a) 0.7 MA/cm² and (b) 3.1 MA/cm². In all images, the grains are highlighted by diffraction contrast created by aligning the beam in the TEM with a major zone axis of the material on one side of the boundary. The GBs in (b) and (c) are indicated with a dashed line.

ably well to the data from thin PLD-grown YBCO films on artificial [001] tilt STO bicrystals. The fact that the data for isolated GBs on RABiTS agrees so well with data for [001] tilt GBs, despite consisting of varying magnitudes of tilt and twist components,¹³ is consistent with previous YBCO bicrystal studies reporting a similar $J_c(\theta)$ dependence for pure [001] tilt, [100] tilt, and [100] twist boundaries.^{1,6} These multiple data sets, derived from different YBCO growth methods, different templates, GBs with different axes of misorientation, yet all consisting of planar GBs, confirm the exponential $J_c(\theta)$ dependence repeatedly reported in the literature.⁵⁻⁷

However, strikingly different results are obtained from GBs isolated in 800 nm thick MOD-grown YBCO films on RABiTS (Fig. 1). These GBs are known to meander strongly about the substrate GBs and through the thickness of the film. There is no longer a consistent trend in J_c as a function of θ . Many of the GBs have greatly enhanced J_c values relative to the traditional exponentially decreasing $J_c(\theta)$ dependence. The most remarkable example is a GB with $\theta \approx 5.5^\circ$ and $J_c = 4.9 \text{ MA/cm}^2$. This value is more than six times higher than indicated by the bicrystal data and nearly the same as J_c within the grain.

To confirm the planar/meandered nature of specific GBs that were measured, cross-sectional TEM specimens were prepared (as described above) from within the $7 \times 20 \mu\text{m}^2$ links for direct observation of the grain boundary structure for several of the samples in Fig. 1. The letters A and C denote two samples with meandered (MOD/RABiTS) and planar (PLD/RABiTS) GBs, respectively. The GB of sample C is revealed in Fig. 2(a), and is macroscopically planar and parallel to the film surface normal. The GB of sample A is revealed in Fig. 2(b), and is highly tilted with respect to the sample normal and meandering, as we have previously reported for similar *ex situ* grown films.^{12,13} For a MOD-grown YBCO film on RABiTS processed similarly to the MOD/RABiTS samples of Fig. 1 (but not presented in Fig. 1), a plan-view TEM specimen was prepared by conventional methods. The observed microstructure is shown in Fig. 2(c), and the YBCO GB is again highly meandered. The amplitude of the meander is significantly smaller than the large amplitudes (several microns) observed by EBSD,^{12,13} revealing the fractal nature of the GB meander and also the large increases in GB area that result from meandering.

The meandered GBs also show remarkably improved critical current densities in applied magnetic fields. In Fig. 3(a), $J_c(H)$ is presented for two of the isolated GBs in Fig. 2: a 7.15° planar GB in a PLD YBCO film and a 6.4° strongly meandered GB in a MOD YBCO film (samples C and B from Fig. 1, respectively). The J_c of the GB from the PLD-grown film is suppressed well below that of the grain out to $\sim 5 \text{ T}$, typical behavior for a GB of this value of θ .⁷ For the meandered GB of the MOD film, J_c of the boundary is only slightly suppressed below the grain out to an applied field of $\sim 2 \text{ T}$. At higher fields, the GB is no longer a barrier to current flow as J_c is limited by vortex depinning within the grains. At 1 T, the J_c of the MOD GB is more than four times higher than that of the PLD GB. The inset to Fig. 3(a) shows four intragrain $J_c(H)$ curves for each of the MOD- and

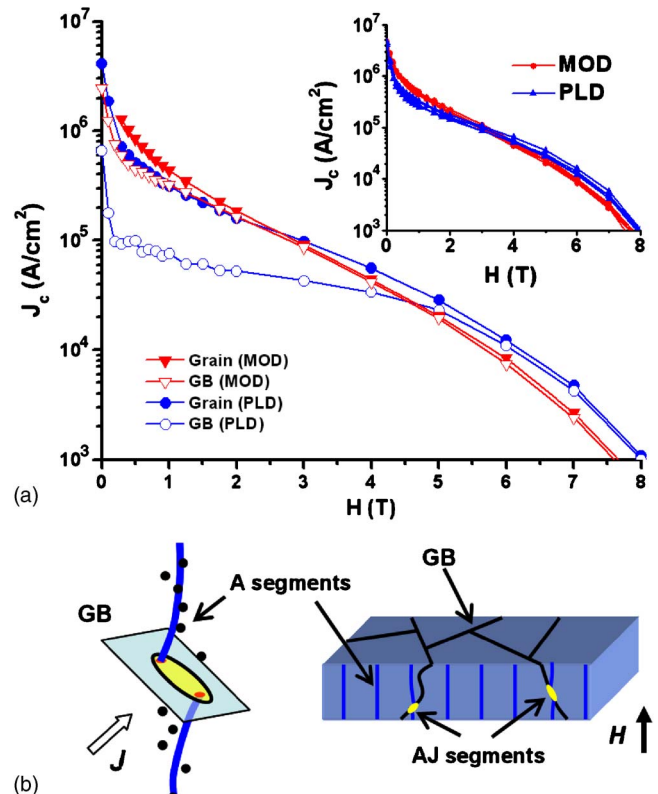


FIG. 3. (Color online) J_c as a function of H for single grains and GBs in YBCO films on RABiTS. (a) $J_c(H)$ is presented for an $\approx 7^\circ$ grain boundary in a PLD-grown film and an $\approx 6.5^\circ$ grain boundary in a MOD-grown film, along with an adjacent grain in each case. The corresponding data in Fig. 1 are highlighted with the letters C and A, respectively. The upper inset shows eight intragrain curves, four each from MOD and PLD films of this work. H was applied parallel to the sample normal (nominally parallel to the YBCO c axis). (b) A schematic of the pinning mechanism concept for GBs highly meandered (tilted) with respect to the sample normal.

PLD-grown YBCO films on RABiTS. The data reveal that the properties of the grain are quite uniform throughout the samples and also very similar for the two different deposition methods, despite their very different GB structures and GB J_c properties.

We believe that two factors are largely responsible for the greatly enhanced J_c across meandered GBs. One is due to the fact that a meandering GB splits a vortex treading the film into two pinned vortex segments in the grains connected by a Josephson string in the GB plane, as illustrated by Fig. 3(b). As shown both theoretically¹⁸ and experimentally,¹⁹ AJ hybrid vortices in the GB plane are pinned weaker than vortices in the grains. However, unlike AJ vortices which lie wholly in the planar GBs, the AJ segments on the meandering GBs cannot easily move under the action of the Lorentz force without pulling strongly pinned A vortex segments in the grains or cutting and reconnecting neighboring flux lines. In this case, weakly pinned AJ segments constitute only a small fraction of vortex length, so the global current transport in a polycrystal with meandering GBs is enhanced by stronger pinning of vortices in the grains.

A recent result consistent with this interpretation is in the study of Durrell *et al.*⁹ Using YBCO films grown by PLD on STO bicrystal substrates (planar GBs), they showed that the characteristic suppression of the GB J_c in applied fields was

ameliorated when the magnetic field was rotated away from the plane of the GB and even disappeared for ϕ greater than a certain threshold ϕ_k , where ϕ is the angle a flux vortex makes with the GB. This observation was attributed to flux cutting, where a short weakly pinned segment within a vortex, which is otherwise strongly pinned, can nevertheless lead to dissipation. Unless a vortex is entirely aligned within the weak pinning channel formed by the grain boundary, the majority of the vortex, in the more strongly pinned grain, will not depin until J_c of the grain is reached. However, flux cutting will occur if the available Lorentz force is sufficient to bend the vortex into an unstable state, at which point the vortex may be displaced through the channel by lengthening until it meets another vortex. In the case of a strongly meandered GB, the angle ϕ at which each vortex intersects the GB is different, and the weak pinning channel formed by the GB is now a highly tortuous path for the AJ vortex segments to walk, which likely results in an increase of the force required to cut a vortex relative to that observed by Durrell *et al.*, leading to further J_c enhancement. A highly meandered GB will also virtually ensure that many vortices will be intersecting the GB at $\phi > \phi_k$, with the result that for these regions of the GB, the J_c across the GB will always be equal to the grain J_c . The slight suppression of the GB J_c below the grain J_c for the meandered GB of Fig. 3(a) is consistent with flux cutting.

A second factor contributing to the enhanced supercurrent across a meandered GB is the increase in GB area,^{20,21} as revealed in Figs. 2(b) and 2(c), which increases the current-carrying cross section. To understand the influence of GB area more explicitly, we measured the current transparency of one GB with no significant meandering in a 250 nm thick YBCO film grown by PLD on a 5° [001] tilt STO bicrystal. Links of a fixed width (w) were patterned across the GB at angles of 0°, 30°, and 60° relative to the normal to the GB plane, resulting in GB areas inside the links of tw , $1.15tw$, and $2tw$, respectively, where t is the thickness of the film. The $J_c(H)$ dependence of these links is shown in Fig. 4. The self-field J_c values of the links (lower inset) show a strong increase in J_c with increasing GB area, consistent with the data of Fig. 2. For the standard measurement geometry where the link is patterned parallel to the GB normal, the GB J_c is suppressed well below that of the grain out to ≈6 T, behavior that is again typical for this GB angle.⁷ As the area of the GB inside the link is increased, the GB curve moves closer to the grain curve, and when the area of the GB in the link is doubled to $2tw$, no suppression of the self-field J_c is observed, and only a slight suppression is observed in applied fields less than 4 T. The curves here corresponding to GB areas of tw and $2tw$ behave very similarly to the GB curves in Fig. 3 of the PLD- and MOD-grown films, respectively. Thus we conclude that the enhanced J_c of meandered GBs has important contributions both from the increased GB area and from enhanced pinning of AJ GB vortex segments by A vortex segments.

CONCLUSION

In conclusion, we have presented a $J_c(\theta)$ study of highly meandered GBs in YBCO. Unlike planar GBs, meandered

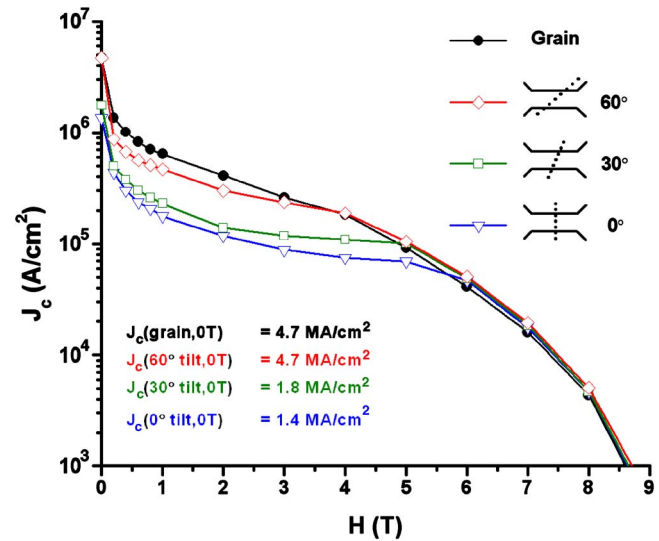


FIG. 4. (Color online) J_c as a function of H for links containing increasing areas of a 5° GB. $J_c(H)$ for three GB links and one intragrain link from a 250 nm thick PLD-grown YBCO film on a 5° [001] tilt SrTiO_3 bicrystal. The three GB links were patterned across the GB at angles of 0°, 30°, and 60° relative to the normal to the GB plane. For the schematics in the legend, the dotted lines represent the GB and the solid lines the edges of the links. J_c was calculated by dividing the critical current of the link by the cross-sectional area of the link.

GBs exhibit greatly enhanced J_c both at self-field and in applied magnetic fields. We conclude that the enhanced J_c of meandered GBs is due to an increase in GB current-carrying cross section and confinement of AJ vortex segments by strongly pinned vortex segments in the grains. We believe that these mechanisms give a possibility to overcome the grain boundary “barrier” in HTS in a much easier way than by Ca overdoping¹⁵ of GBs.

ACKNOWLEDGMENTS

This work was funded by the Department of Energy Office and by the Air Force Office of Scientific Research.

- ¹H. Hilgenkamp and J. Mannhart, Rev. Mod. Phys. **74**, 485 (2002).
- ²A. Gurevich and E. A. Pashitskii, Phys. Rev. B **57**, 13878 (1998).
- ³M. A. Schofield, M. Beleggia, Y. M. Zhu, K. Guth, and C. Jooss, Phys. Rev. Lett. **92**, 195502 (2004).
- ⁴D. Larbalestier, A. Gurevich, D. M. Feldmann, and A. Polyanskii, Nature (London) **414**, 368 (2001).
- ⁵D. Dimos, P. Chaudhari, and J. Mannhart, Phys. Rev. B **41**, 4038 (1990).
- ⁶D. M. Feldmann, D. C. Larbalestier, D. T. Verebelyi, W. Zhang, Q. Li, G. N. Riley, Jr., R. Feenstra, A. Goyal, D. F. Lee, M. Paranthaman, D. M. Kroeger, and D. K. Christen, Appl. Phys. Lett. **79**, 1 (2001).
- ⁷D. T. Verebelyi, D. K. Christen, R. Feenstra, C. Cantoni, A. Goyal, D. F. Lee, M. Paranthaman, P. N. Arendt, R. F. DePaula, J. R. Groves, and C. Prouteau, Appl. Phys. Lett. **76**, 1755 (2000).
- ⁸A. Diaz, L. Mechin, P. Berghuis, and J. E. Evetts, Phys. Rev. Lett. **80**, 228 (1998).
- ⁹J. H. Durrell, M. J. Hogg, F. Kahlmann, Z. H. Barber, M. G. Blamire, and J. E. Evetts, Phys. Rev. Lett. **90**, 247006 (2003).
- ¹⁰X. Y. Song, G. Daniels, D. M. Feldmann, A. Gurevich, and D. Larbalestier, Nat. Mater. **4**, 470 (2005).
- ¹¹P. C. McIntyre, M. J. Cima, and M. F. Ng, J. Appl. Phys. **68**, 4183 (1990).
- ¹²D. M. Feldmann, D. C. Larbalestier, T. G. Holesinger, R. Feenstra, A. A. Gapud, and E. D. Specht, J. Mater. Res. **20**, 2012 (2005).
- ¹³D. M. Feldmann, T. G. Holesinger, C. Cantoni, R. Feenstra, N. A. Nelson, D. C. Larbalestier, D. T. Verebelyi, X. Li, and M. Rupich, J. Mater. Res. **21**, 923 (2006).

- ¹⁴T. G. Holesinger, P. N. Arendt, R. Feenstra, A. A. Gapud, E. D. Specht, D. M. Feldmann, and D. C. Larbalestier, *J. Mater. Res.* **20**, 1216 (2005).
- ¹⁵G. Hammerl, A. Schmehl, R. R. Schulz, B. Goetz, H. Bielefeldt, C. W. Schneider, H. Hilgenkamp, and J. Mannhart, *Nature (London)* **407**, 162 (2000).
- ¹⁶A. Goyal, S. X. Ren, E. D. Specht, D. M. Kroeger, R. Feenstra, D. Norton, M. Paranthaman, D. F. Lee, and D. K. Christen, *Micron* **30**, 463 (1999).
- ¹⁷M. W. Rupich, D. T. Verebelyi, W. Zhang, T. Kodenkandath, and X. Li, MRS Bull. **29**, 572 (2004).
- ¹⁸A. Gurevich and L. D. Cooley, *Phys. Rev. B* **50**, 13563 (1994).
- ¹⁹A. Gurevich, M. S. Rzchowski, G. Daniels, S. Patnaik, B. M. Hinaus, F. Carillo, F. Tafuri, and D. C. Larbalestier, *Phys. Rev. Lett.* **88**, 097001 (2002).
- ²⁰W. Zhang, E. A. Goodilin, and E. E. Hellstrom, *Supercond. Sci. Technol.* **9**, 211 (1996).
- ²¹J. Mannhart and C. C. Tsuei, *Z. Phys. B: Condens. Matter* **77**, 53 (1989).